

Mechanisms of Non-Factual Hallucination in Language Models

Lei Yu^{1,*}, Meng Cao^{2,3,*}, Jackie Chi Kit Cheung^{2,3}, Yue Dong⁴

¹Department of Computer Science, University of Toronto

²School of Computer Science, McGill University

³Mila – Québec AI Institute

⁴University of California, Riverside

jadelei@cs.toronto.edu

{meng.cao@mail,jcheung@cs}.mcgill.ca

yue.dong@ucr.edu

Abstract

State-of-the-art language models (LMs) sometimes generate *non-factual hallucinations* that misalign with world knowledge. Despite extensive efforts to detect and mitigate hallucinations, understanding their internal mechanisms remains elusive. Our study investigates the mechanistic causes of hallucination, specifically non-factual ones where the LM incorrectly predicts object attributes in response to subject-relation queries. With causal mediation analysis and embedding space projection, we identify two general mechanistic causes of hallucinations shared across LMs of various scales and designs: 1) insufficient subject attribute knowledge in lower layer MLPs, and 2) failing to select the correct object attribute in upper layer attention heads and MLPs. These two mechanisms exhibit varying degrees of subject-object association, predictive uncertainty and perturbation robustness. Additionally, we scrutinize LM pre-training checkpoints, revealing distinct learning dynamics for the two mechanistic causes of hallucinations. We also highlight how attribution features from our causal analysis can effectively construct hallucination detectors. Our work proposes a mechanistic understanding of LM factual errors.¹

1 Introduction

Language models (LMs) serve as repositories of substantial knowledge (Petroni et al., 2019; Jiang et al., 2020; Srivastava et al., 2023) through their parametric knowledge gained from pre-training. However, they are susceptible to generating “hallucinations” that contain factual errors. At the level of logit predictions, these hallucinations often display a pattern similar to factual generations. For example, LMs have been observed to produce seemingly confident completions that are, in reality, hallucinations (Dong et al., 2022; Zhang et al., 2023b).

To understand how hallucinations differ from factual outputs and whether they are uniformly generated or equally challenging to fix, thorough analysis tools that monitoring the information flow are required, extending beyond merely last-layer predictions (Kaddour et al., 2023). However, research on understanding the internal mechanisms of hallucination generation is limited. Most efforts have focused on detecting and mitigating hallucinations (Elaraby et al., 2023; Mündler et al., 2023; Manakul et al., 2023; Zhang et al., 2023a), treating the LM as a black box and devising methods based on external features like predictive uncertainty (Xiao and Wang, 2021; Varshney et al., 2023) and logical consistency (Cohen et al., 2023). Unfortunately, these approaches provide no insights into the internal mechanisms of factual errors and have demonstrated unreliability or conveyed contradictory signals (Turpin et al., 2023).

In contrast, interpretability research, which probes the internal mechanisms of transformers in white-box settings, has recently garnered significant attention for analyzing which components are helpful in identifying factual predictions. It has identified several critical model “components” (e.g., attention heads, feedforward layers) related to knowledge flow that are essential for answering questions accurately (Lu et al., 2021; Dai et al., 2022; Meng et al., 2022a; Geva et al., 2023). However, it remains a question whether the results of mechanistic interpretability on factual predictions can generalize to hallucinations. Specifically, it is unknown which model components deviate from normal functioning to cause hallucinations. Localizing the source of factual errors in LMs may help us design targeted and efficient methods to mitigate hallucinations (e.g., by editing a small set of model weights identified as causing hallucinations), which is particularly important as the model size and the training cost of LMs are rapidly increasing.

In this study, we employ mechanistic inter-

*Equal contribution.

¹Our code and data are available at: https://github.com/jadelei/lm_hallucination_mechanisms.

pretability (Olah, 2022) to investigate the origins and manifestation of non-factual hallucinations in LMs. We use two established interpretability methods, causal mediation analysis (Pearl, 2001; Vig et al., 2020) and embedding space projection (Geva et al., 2022b; Dar et al., 2023) in our specially designed setups on non-factual hallucination data, aiming to assess the influence of model components on hallucinating predictions. Through extensive analyses on LMs of various sizes and architectures (Llama-2, GPT-J, GPT-2-XL), we obtain converging evidence that there exist two groups of crucial components for factually incorrect predictions: 1) the multi-layer perceptrons (MLPs) in lower transformer layers, 2) the attention heads and MLPs in upper transformer layers.

Figure 1 illustrates two distinct scenarios where the identified hallucinating components exhibit different behaviors. In some instances, lower-layer MLPs function normally, successfully retrieving semantic attributes about queried entities, while upper-layer attention heads and MLPs struggle to distinguish the most relevant attributes that lead to the correct answer. In other cases, the model fails to execute its fact-recalling pipeline at the beginning, extracting no useful information from lower-layer MLPs. We also observe that these two hallucination mechanisms have varying external manifestations, distinguishable by their levels of subject-object association strengths, robustness to input perturbations, and model predictive uncertainty. Following the discoveries by Akyürek et al. (2022); Zhou et al. (2023) regarding the significant role of LM pre-training in acquiring factual knowledge, we also examined the impact of pre-training on the various types of hallucinations we have identified. Our findings are significant: early-site MLPs and late-site attentions form a two-step pipeline for fact recall that emerges progressively during pre-training, and failing to develop either step can result in hallucinations.

In addition to providing internal knowledge flow analysis that exhibits high correlations with external features, which helps us understand how different types of hallucinations behave during various stages of pre-training, our work also demonstrates a practical application: mechanistic interpretability features can be employed to detect the presence of factual errors in language models (LMs). This research offers the first mechanistic explanation of LM factual errors as systematic modular failures, fostering research on model explainability and hal-

lucination mitigation.

2 Related Work

Factual knowledge in language models. The exploration of knowledge tracing within Language Models (LMs) has gained substantial attention lately, with researchers investigating specific layers (Wallat et al., 2020; Geva et al., 2021; Meng et al., 2022a) and neurons (Dai et al., 2022) responsible for storing factual information. This line of inquiry extends to techniques for model editing (De Cao et al., 2021; Mitchell et al., 2021; Meng et al., 2022b) and inference intervention (Hernandez et al., 2023; Li et al., 2023). Recent advancements by Geva et al. (2023); Yu et al. (2023) identify crucial LM components that form an internal pipeline for factual information transfer. Our framework complements existing research by offering an additional perspective on LM factual knowledge processing, revealing that compromised factually relevant modules can lead to hallucinations.

Hallucinations. Language models are susceptible to generating hallucinations that can be *unfaithful* (i.e. deviating from the source input provided by users) or *non-factual* (i.e. contradicting established world knowledge) (Cao et al., 2022a; Ji et al., 2023; Zhang et al., 2023b). Here, we focus on the latter type of hallucination. Existing studies propose various methods to detect or mitigate hallucinations, leveraging features such as internal activation patterns (Yuksekgonul et al., 2023; Li et al., 2023), predictive confidence (Cao et al., 2022a,b; Varshney et al., 2023), and generation consistency (Mündler et al., 2023; Manakul et al., 2023; Zhang et al., 2023a).

Mechanistic interpretability. Mechanistic interpretability (Olah, 2022; Nanda, 2023) is an evolving research area. Recent works employ projections to the vocabulary (Geva et al., 2022b,a; Nostalgebraist, 2020; Katz et al., 2024) and interventions in transformer computation (Finlayson et al., 2021; Haviv et al., 2022; Stolfo et al., 2023; Ghandeharioun et al., 2024) to study LM inner workings. Similar techniques have been applied to explore neural network learning dynamics (Nanda et al., 2022) and discover sparse computational graphs for specific tasks (Wang et al., 2022; Conmy et al., 2023). Leveraging multiple mechanistic interpretability methods, our study provides a principled account for non-factual hallucinations.

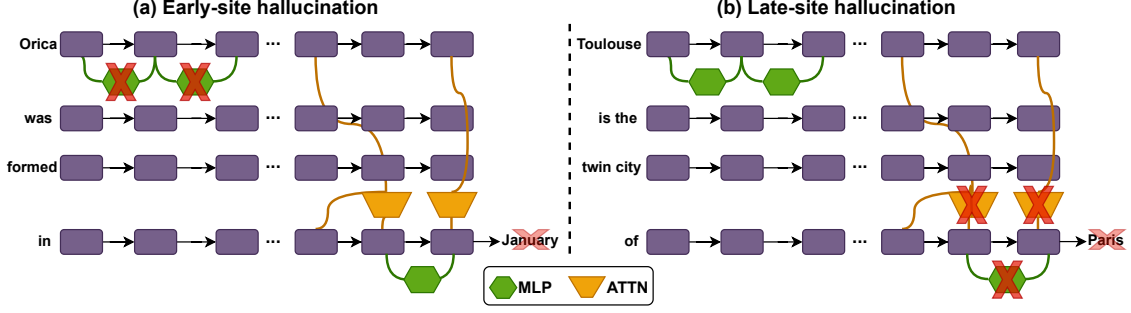


Figure 1: **Our main finding of two non-factual hallucination mechanisms.** Left (a): The **early-site hallucinations** are caused by lacking general knowledge of the subject in lower layer MLPs of transformer LMs – in this case, the model fails to retrieve useful information about the entity (e.g., *Orica*, an Australian-based multinational corporation) to generate the correct object attribute (e.g., *Australia*), and therefore outputs a highly irrelevant prediction (January). Right (b): The **late-site hallucinations** are caused by the failure of upper layer attention heads and MLPs to identify the most relevant object to the given subject and relation – in this case, the model is able to retrieve related information about the subject (e.g., *Toulouse*, a French city) from lower layer MLPs, but cannot distinguish the irrelevant yet strongly associated attributes (e.g., *Paris*) from the correct answers (e.g., *Bologna/Chongqing/Atlanta*). We found that these two types of hallucinations can be distinguished by the relative causal contribution to model predictions between lower and upper layer LM components.

3 Background and Notation

We start by providing a detailed description of the inference pass of decoder-only transformer-based LMs. An auto-regressive transformer, denoted as G , maps an input sequence of tokens $u = [w_1, \dots, w_T]$, represented by input token embeddings $E(u) = [e_1, \dots, e_T]$, into a probability distribution over the vocabulary for next-token prediction. Within the transformer, the i -th token is represented as a series of hidden states $h_i^{(l)}$ where at each layer l , the model computes and adds the intermediate embeddings by two modules from $h_i^{(l-1)}$: 1) an aggregated **multi-head self-attention module** output $a_i^{(l)} = W_o([a_i^{(l,0)}, \dots, a_i^{(l,K)}])$, where $a_i^{(l,k)}$ is the output of the k -th attention head at layer l (with K heads in total) for the i -th token, and W_o is a linear transformation; 2) a **multi-layer perceptron (MLP)** output $m_i^{(l)} = f_{\text{MLP}}^{(l)}(h_i^{(l-1)} + a_i^{(l)})$ at layer l . Putting together, the hidden representation $h_i^{(l)}$ is computed as: $h_i^{(l)} = h_i^{(l-1)} + a_i^{(l)} + m_i^{(l)}$. Let $H = \{h_i^{(l)}\}$ be the set of $T \times L$ token hidden states across all layers (following Elhage et al. (2021)), we shall call them the **residual stream outputs**, $A = \{a_i^{(l)}\}$ be the set of $T \times L$ **attention outputs**, and $M = \{m_i^{(l)}\}$ be the set of $T \times L$ **MLP outputs**. We aim to investigate which intermediate hidden representations $z \in Z = H \cup A \cup M$ are causally contributing to the generation of a factually incorrect entity. For further details on transformers, see Vaswani et al. (2017).

4 Mechanisms of Hallucinations

4.1 Causal tracing of factual errors

Method. The intermediate hidden states H produced by G during model inference form a causal dependency graph (Pearl, 2001) that contains many paths from the input sequence to the output (next-token prediction), and we wish to understand if there are specific hidden states that are more important than others when producing a hallucination. This is a natural case for *causal mediation analysis*, which quantifies the contribution of intermediate variables in causal graphs. For more information about causal mediation analysis of language models, see Vig et al. (2020).

We adapt the framework of Meng et al. (2022a) to locate LM components that cause factual errors via the task of factual open-domain questions on structured queries. In particular, given a fact represented as a subject-relation-object triple (s, r, o) , we provide an LM G with a query prompt u containing (s, r) (e.g., “Toulouse is the twin city of ___”) with o as a true continuation (e.g., “Atlanta”). We examine the cases where G predicts an incorrect object o' as the next token(s) given u , and aim to locate which intermediate hidden states in the computation graph of G led to the hallucination. We consider G to be a “corrupted” model with certain modules failing to compute the “clean” representations that could otherwise lead to the correct answer o , and measure the contribution of each module through three model runs:

1. In the **hallucination run**, we pass u into G and extract all intermediate hidden representations Z as defined in Section 3, and compute the log likelihood ratio $y = \log \frac{p(o'|E(u))}{p(o|E(u))}$ between the true and hallucinated objects, which quantifies the “degree of hallucination” of G . For a hallucinating prediction, we would observe $y > 0$.
2. In the **mitigation run**, we follow Meng et al. (2022a) and add a Gaussian noise $\epsilon \sim \mathcal{N}(0, 1)$ to the input token embeddings $E(u)$, so that when taking the intervened $E^*(u) = E(u) + \epsilon$ as inputs, the log-likelihood ratio between the hallucinated and the factual object would decrease (i.e., we only take noises with $y_* = \log \frac{p(o'|E^*(u))}{p(o|E^*(u))} < y$, indicating that the model becomes more “truthful” after noise injections). We again extract all intermediate hidden representations, denoted as Z^* .
3. In the **mitigation-with-hallucination-state run**, we run G on u with perturbed input embeddings $E^*(u)$ as in the mitigation run, and hook G by forcing a particular hidden representation $z^* \in Z^*$ to be the hidden representation z during the hallucination run. We then compute the log likelihood ratio $y_{E^*,z} = \log \frac{p(o'|E^*(u),z)}{p(o|E^*(u),z)}$ to see how it changes compared to step 2.

Following previous work in causal mediation analysis (Vig et al., 2020; Finlayson et al., 2021; Meng et al., 2022a), we define the **causal indirect effect** $IE(z; y, u, \epsilon) = y_{E^*,z} - y_*$ of an intermediate hidden representation z as the decrease in the degree of hallucination after mitigating a single hidden state. Averaging over a set of factual queries and a sample of noises for each query, we obtain the average indirect effect (AIE) for each z and its corresponding model component.

Experiments. We collect a set of factual knowledge queries from the ParaRel (Elazar et al., 2021) dataset of cloze-style factual knowledge queries. Each example in ParaRel contains a knowledge tuple $t_c = (s, r, o_c)$ and a prompt generated from hand-curated templates. We evaluated three widely used pretrained LMs with different layouts: 1) Llama-2-7B-chat (32 layers, 7B parameters, fine-tuned on instruction following) (Touvron et al., 2023), 2) GPT-J (28 layers, 6B parameters) (Wang

and Komatsuzaki, 2021), and 3) GPT-2-XL (48 layers, 1.5B parameters) (Radford et al., 2019). For each prompt u , we compute the LM predicted conditional probability $p(o|E(u))$ of the next token continuation, where o is taken from the collection of all capitalized alphabetical tokens in the model vocabulary. To resolve the ambiguity issue where a query may allow multiple correct answers, we define hallucinations as the cases where the LM assigns the highest probability to a token o' that is neither the suffix of the true object o_c nor the suffix of any other objects of the subject-relation pair (s, r) returned by a WikiData API query search.²

Results. We compute the average causal indirect effect over queries from ParaRel for hidden states $z \in Z$ across various sentence positions and transformer layers. Figure 2 shows the AIE distributions for three model components of Llama-2-7B: the residual stream, the attention heads, and the MLPs. We observe two groups of hidden states yielding the highest attribution scores towards incorrectly predicted objects: 1) the hidden states of the subject tokens at lower transformer layers by MLPs, and 2) the hidden states of the last relation token at upper transformer layers by MLPs and attention heads. We observe similar causal effect distributional patterns for GPT models as well (see Appendix B.2 for additional results). Geva et al. (2023) recently show that lower layer MLPs and upper layer attention heads are two most crucial LM components for successful factual knowledge recalling. Our causal tracing results not only confirm their finding from a contrapositive perspective, but also reveal an additional component (upper layer MLPs) as an important source of hallucinations.

Early- vs. late-site hallucination. Based on the findings above, we hypothesize that there are two different “mechanisms” that may cause non-factual hallucinations, as illustrated in Figure 1: 1) the LM fails to retrieve correct information about the subject from lower layer components, and 2) the LM successfully retrieves some subject attributes from lower layer components, but the upper layer components fail to distinguish the correct object(s) among retrieved ones. In particular, let L be the number of transformer layers of an LM, we define *early-site components* as attention heads and MLPs located in the first half of LM’s layers ($1 \leq l \leq \frac{L}{2}$),

²See Appendix A for more details about dataset construction.

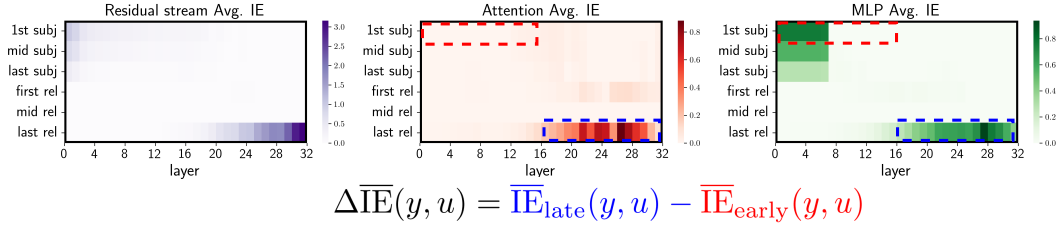


Figure 2: **Average Indirect Effect (AIE)** of hidden representations produced by individual model components to non-factual hallucinations over ParaRel queries that are incorrectly answered by Llama-2-7b-chat. The relative indirect effect metric $\Delta \overline{\text{IE}}(y, u)$ of distinguishing early-site and late-site hallucinations is defined as the difference between the mean AIE of 1) the hidden representations of the last relation token by upper layer attentions/MLPs (blue dashed boxes), and 2) the hidden representations of the first subject token by lower layer attentions/MLPs (red dashed boxes).

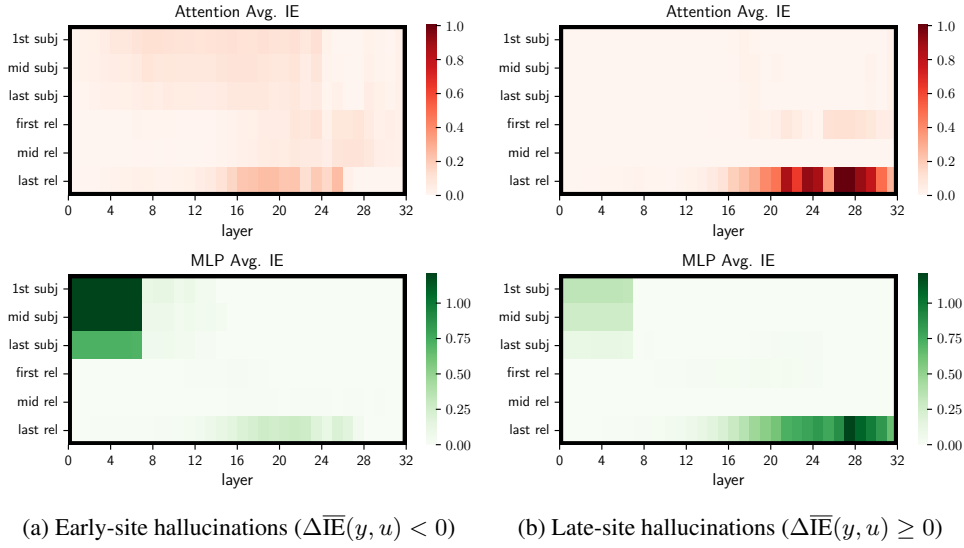


Figure 3: **Average Indirect Effect (AIE)** of individual model components for (a) early-site (left column) and (b) late-site (right column) non-factual hallucinations.

and *late-site components* as those located in the second half of LM’s layers ($\frac{L}{2} < l \leq L$). We then define the **relative indirect effect** between intermediate representations by early- and late-site model components as:

$$\Delta \overline{\text{IE}}(y, u) = \overline{\text{IE}}_{\text{late}}(y, u) - \overline{\text{IE}}_{\text{early}}(y, u) \quad (1)$$

$$= \frac{2}{L} \left[\sum_{l=1+\frac{L}{2}}^L \overline{\text{IE}}(z_T^{(l)}, y, u) - \sum_{l=1}^{\frac{L}{2}} \overline{\text{IE}}(z_0^{(l)}, y, u) \right], \quad (2)$$

where $\overline{\text{IE}}_{\text{early}}(y, u)$ is the average indirect effect of early-site intermediate representations of the first subject token w_0 (hidden states in blue dashed boxes in Figure 2), and $\overline{\text{IE}}_{\text{late}}(y, u)$ is the average indirect effect of late-site intermediate representations of the last relation token w_T of u (hidden states in red dashed boxes in Figure 2). We categorize a hallucination (u, o, o') as **early-site** if its lower layer hidden representations have stronger

AIEs (i.e. $\Delta \overline{\text{IE}}(y, u) < 0$), and otherwise categorize it as **late-site** (i.e. $\Delta \overline{\text{IE}}(y, u) \geq 0$). We found that early-site and late-site hallucinations have very different AIE distributions: as shown in 3, while most components that contribute significantly to early-site hallucinations are located in lower layers when processing subject tokens, late-site hallucinations are mostly caused by components concentrated in upper layers when processing the relation tokens.

External manifestations of hallucination mechanisms. To verify that our categorization of hallucinations is not a fabricated dichotomy based solely on internal computation patterns, we next investigate whether there are any external features that can be leveraged to distinguish the two types of hallucinations. We consider the following features of query data and model predictions: the **subject-**

Statistics	Early-site hall.	Late-site hall.
Amount	(1945 / 31.9%)	(4152 / 68.1%)
s - o assoc.	0.40	0.88
s - o' assoc.	0.85	2.03
Robustness	0.78	0.51
Uncertainty	4.39	4.17

Table 1: External data and Llama-2-7b prediction features for two types of non-factual hallucination.

object association strength is measured as the inner product between the input layer embeddings of a subject s and a true object o or a hallucinating object o' ; the **robustness** of a predicted object o' is measured as the percentage of Gaussian noise injected during the mitigation run in section 4.1 which, after being added to the input embeddings, fails to make the model prefer the true answer o over o' (i.e., $y_* < 0 < y$); the **uncertainty** of model prediction is measured by the entropy of the conditional next-token distribution $p(o|u)$. Table 1 summarizes the external measurements. We found that 1) subjects of late-site hallucinations (e.g., *Toulouse*) often have hallucinating objects (e.g., *Paris*) of much stronger association strengths than true objects (e.g., *Bologna*), so that the model fail to “offset” the prior propensity of model predicting o' upon seeing s . Subjects of early-site hallucinations (e.g., *Orica*), on the other hand, often have much weaker associations with both true (e.g., *Australia*) and hallucinating (e.g., *January*) objects; 2) late-site hallucinations are significantly less robust under input perturbations, probably because the model has already retrieved the correct object from early layers and is just “one step away” from distinguishing it; 3) the model is less certain about its predictions when generating early-site hallucinations, a pattern that is consistent with previous findings that epistemic hallucinations are often associated with high predictive uncertainty (Xiao and Wang, 2021).

4.2 Inspection via embedding space projection

In this section, we provide further evidence of the mechanistic difference between early- and late-site hallucinations by looking at the information that each model component writes into the residual stream during inference.

Method. As Section 3 suggests, each attention or MLP module at layer l contributes to the model prediction by adding its output hidden state into

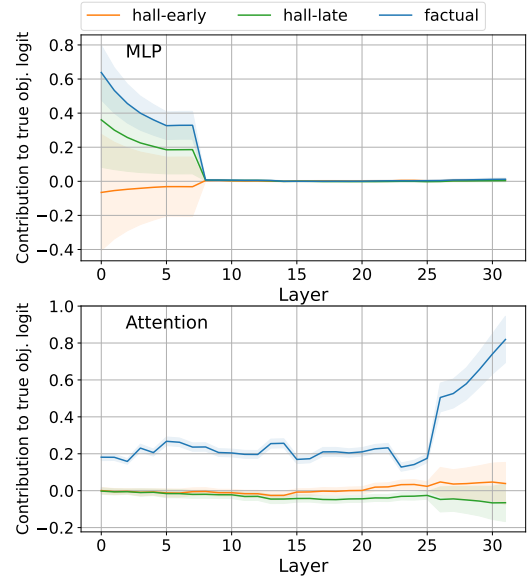


Figure 4: Average dot product between true object embedding and intermediate hidden representations by components of Llama-2-7b in each layer.

the embeddings $h_i^{(l-1)}$ produced by the previous layer. Recent work shows that the encoded knowledge of a module can be interpreted by applying the final-layer language model head projection (i.e. dot product) to its intermediate output hidden state, thereby obtaining a distribution over the vocabulary (Geva et al., 2022b; Dar et al., 2023). For each example of model hallucination (u, o, o') , we use this method by first extracting the intermediate outputs $z \in A \cup M$ of all MLPs and attention modules, and then taking the dot product $\tilde{p}(z, o) = z^T e_o$ between z and the row vectors corresponding to o in the final projection layer. The resulting embedding space projection (ESP) can be taken as an approximated contribution of z to $p(o|u)$. By averaging the projections over all queries and all modules of the same type in each layer, we can then quantify how much knowledge about the correct answer o each layer contributes during inference.

Results. We compute the layerwise MLP and attention projections for the true objects averaged over three groups of queries: 1) factual answers (i.e. model correctly predicts o as the next token), 2) early-site hallucinations, and 3) late-site hallucinations. Figure 4 shows the results. We notice that 1) only lower layer MLPs write information about the true answer into the residual stream, and importantly, the contributions of lower layer MLPs are similar for late-site hallucinations and correctly answered queries, while being much less when the

model generates early-site hallucinations. 2) For both types of hallucination, the self-attention components, particularly those in upper layers, write significantly less useful information compared to factually correct answers. Similar patterns observed in GPT models can be found in Appendix B.4.

Taken together, our analysis suggests that 1) *early-site MLPs, late-site self-attentions and late-site MLPs are the most crucial LM components of causing hallucinations*, and 2) *lower layer MLPs and upper layer attentions/MLPs do not always break down simultaneously, thus leading to two distinct mechanisms of LM factual errors*.

5 Tracing LM Hallucinations During Pretraining

We have identified two mechanisms of non-factual hallucinations in LMs. In this section, we design experiments with the goal of understanding how these hallucinations emerge during model pretraining. For example, do early-site and late-site hallucinations exhibit different learning patterns that contribute to their distinctions? We also aim to explore why the crucial early-site MLP and late-site attention components fail to “develop” properly.

Data and models. To study language model hallucinations during pretraining, we evaluate the Pythia model suite (Biderman et al., 2023) on ParaRel. Pythia is a set of pretraining checkpoints for a family of autoregressive LMs trained on public data in the exact same order. We first take the last checkpoint of Pythia with 1.4 billion parameters and repeat the same evaluation and filtering processes for other LMs on ParaRel dataset described in section 4.1, and then perform causal mediation analysis on incorrectly answered queries to get AIEs for attention heads and MLPs, and categorize the queries into early-site and late-site hallucinations based on Equation 2. We then evaluate and get intermediate hidden states for all queries on 32 Pythia-1.4B pretraining checkpoints evenly distributed across model learning history.³

Development of factual association pipeline. We replicate the embedding space projection (ESP) experiments in section 4.2 on Pythia-1.4b checkpoints and compare the results across pretraining steps. For each Pythia-1.4B checkpoint, we first take the ESP onto the true object tokens for 1)

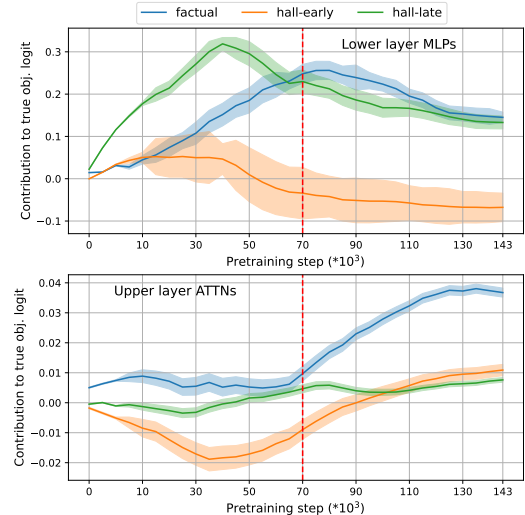


Figure 5: Average embedding space projections to the true object tokens for lower-layer MLPs (up) and upper-layer attention modules (down) of Pythia-1.4b pretraining checkpoints. The red vertical line indicates a “phase change” when the lower layer MLPs finish their learning, and upper layer attention heads start to develop.

MLPs in the first 12 out of 24 transformer layers, and 2) attention heads in the last 12 layers, and then compute the average ESP for the sets of factual, early-site hallucination and late-site hallucination queries (categorized based on prediction results by the last model checkpoint). Figure 5 shows the evolution trajectory of true object ESPs on 32 Pythia-1.4b checkpoints. We notice that 1) the learning dynamics of MLPs between late-site hallucination and factual queries are very similar, where they gradually learn to produce positive ESPs to the true object prediction roughly during the first half of pretraining. For early-site hallucinations, the MLPs instead learn to make negative ESPs, again suggesting their lack of true subject knowledge. 2) The upper-layer attentions of Pythia only learn to produce high ESPs for factual queries. Moreover, the attention modules will not learn to distinguish true objects until the early-site MLPs have grown mature (~ 70 -th pretraining step). Taken together, our results suggest that *the early-site MLPs and late-site attentions together form a two-step pipeline of fact recall that emerges progressively during pretraining, and failing to develop either of them will lead to non-factual hallucinations*.

6 Application to Hallucination Detection

We have demonstrated that mechanistic interpretability methods can reveal causes of LM factual

³See Appendix C for details of Pythia evaluation.

errors when we know that the model is hallucinating. In this section, we further show that the causal attribution features in our previous analyses can also predict whether an LM is generating hallucinations.

Data. We study non-factual hallucinations by GPT2-XL⁴ on three datasets: 1) the **ParaRel** dataset used in section 4, 2) the **Natural Questions** dataset (Kwiatkowski et al., 2019) that consists of Google search engine queries annotated with answers and supporting Wikipedia pages, and 3) the **TruthfulQA** dataset by Lin et al. (2022) consisting of adversarially constructed commonsense reasoning questions to measure whether an LM is truthful in generating answers. We follow the multiple-choice evaluation scheme in question answering and ask GPT2-XL to compute the conditional log-likelihood of every candidate answer. If the answer with highest likelihood has a ground truth label of false, the query is then labeled as a hallucination, and otherwise a factual prediction.

Methods. We study the following classification problem: given a query u and a next-word prediction o by a language model, we wish to predict whether the model is hallucinating or not. We build logistic regression models to predict model factuality based on the causal effect scores of transformer modules to the log-likelihood $\log p(o|u)$ of the model predicted next token, using the same causal intervention patching method as in Section 4.1. Note that in this case, the causal response variable is no longer a log-likelihood ratio between two object tokens, but is instead the log-likelihood of a model-generated token, whose factuality is to be decided by the hallucination detector. We compute the AIE for each neuron in the intermediate outputs of the attention, MLP and residual stream modules across 48 layers, and concatenate the arrays of AIE scores of three modules to get a single 4,800-dimensional feature vector. Since performing causal mediation analysis over individual neurons is very expensive, we adopt the gradient-based approximation method of causal mediation effect by (Nanda, 2023) to accelerate computations⁵.

⁴We encountered GPU memory issues when implementing gradient-based baselines and causal approximations on larger LMs, so here we focused on GPT2-XL and leave experiments on other LMs for future work.

⁵See Appendix D for details of the causal effect approximation method.

	ParaRel	NaturalQA	TruthfulQA
Random	50.0	50.0	50.0
LHS	62.1	56.6	50.4
Activation	67.8	62.6	52.0
Gradient	68.8	66.1	53.8
Grad. X Act.	68.9	68.3	60.1
IG	69.9	67.4	53.2
Causal IE	70.7	69.8	60.8

Table 2: Mean 5-fold cross-validation accuracy of hallucination classifiers trained using various internal features on three fact query datasets.

Baselines. We also test baseline logistic regression models using a suite of non-causal internal features that have been shown to be indicative of LM hallucinations: 1) the last-layer hidden state of the last token of the input sequence, which the model uses directly to generate the next token (Zhou et al., 2021); 2) the activation values (Li et al., 2023); 3) the gradients (De Cao et al., 2021) with respect to $\log p(o|u)$; 4) the activation * gradient values (Tang et al., 2022) with respect to $\log p(o|u)$; and 5) the Integrated Gradient (Sundararajan et al., 2017) with respect to $\log p(o|u)$. For baselines (2)-(4), we compute features for the same set of intermediate neurons as for the causal effect-based classifiers, so that the dimensions of baseline input feature vectors are the same as the IE-based feature vectors.

Results. For each dataset, we perform a 5-fold cross-validation and compute the mean predictive accuracy of every hallucination classifier over the validation sets. Table 2 summarizes the results. We found that the causal indirect effect features best predict model hallucinations on all datasets, consistently exceeding all baseline models. Notably, all baselines except IG only make use of internal information without input perturbations, so their inferior performance compared to AIE suggests that counterfactual interventions of model inference process in causal mediation analysis are crucial for locating crucial components of causing factual errors. The IG baseline, as suggested by Meng et al. (2022a), is often over-sensitive to input textual artifacts (e.g. rare words and typos), and therefore yields much less reliable predictions on the two QA datasets with diverse input formats.

7 Conclusion

Through interpretability analysis, we identified two causes of language model non-factual hallucina-

tions: 1) insufficient attribute knowledge in lower layer MLPs and 2) flawed object selection in upper layer attentions and MLPs. We also revealed distinguishing properties in data and model predictions, along with divergent pre-training trajectories for the two mechanistic types of hallucination. Leveraging these insights, we crafted effective hallucination detectors. Our work establishes a mechanistic understanding of LM factual errors, and may inspire future research on explainable approaches of hallucination mitigation.

8 Limitation

Our study bears several limitations. Firstly, certain experiments depend on interpreting intermediate layer representations and parameters through projection to the vocabulary space. While widely used, this method only approximates the encoded information of model components, particularly in early layers. Secondly, our focus on non-factual hallucinations with simple input sequences may not fully capture real-world LM behavior. Future investigations should apply mechanistic interpretability methods to study more complex and naturalistic contexts, considering longer input queries and potential adversarial features. Thirdly, we did not explore methods to reduce LM hallucinations based on insights gained from our mechanistic analysis. Future work may consider develop efficient hallucination mitigation methods by performing targeted weight editing or inference time intervention on crucial model components identified in this study.

References

- Ekin Akyürek, Tolga Bolukbasi, Frederick Liu, Binbin Xiong, Ian Tenney, Jacob Andreas, and Kelvin Guu. 2022. Towards tracing knowledge in language models back to the training data. In *Findings of the Association for Computational Linguistics: EMNLP 2022*, pages 2429–2446.
- Stella Biderman, Hailey Schoelkopf, Quentin Gregory Anthony, Herbie Bradley, Kyle O’Brien, Eric Hallahan, Mohammad Aflah Khan, Shivanshu Purohit, USVSN Sai Prashanth, Edward Raff, et al. 2023. Pythia: A suite for analyzing large language models across training and scaling. In *International Conference on Machine Learning*, pages 2397–2430. PMLR.
- Meng Cao, Yue Dong, and Jackie Cheung. 2022a. [Hallucinated but factual! inspecting the factuality of hallucinations in abstractive summarization](#). In *Proceedings of the 60th Annual Meeting of the Association for Computational Linguistics (Volume 1: Long Papers)*, pages 3340–3354, Dublin, Ireland. Association for Computational Linguistics.
- Meng Cao, Yue Dong, Jingyi He, and Jackie Chi Kit Cheung. 2022b. [Learning with rejection for abstractive text summarization](#). In *Proceedings of the 2022 Conference on Empirical Methods in Natural Language Processing*, pages 9768–9780, Abu Dhabi, United Arab Emirates. Association for Computational Linguistics.
- Roi Cohen, May Hamri, Mor Geva, and Amir Globerson. 2023. Lm vs lm: Detecting factual errors via cross examination. *arXiv preprint arXiv:2305.13281*.
- Arthur Conmy, Augustine N Mavor-Parker, Aengus Lynch, Stefan Heimersheim, and Adrià Garriga-Alonso. 2023. Towards automated circuit discovery for mechanistic interpretability. *arXiv preprint arXiv:2304.14997*.
- Damai Dai, Li Dong, Yaru Hao, Zhifang Sui, Baobao Chang, and Furu Wei. 2022. Knowledge neurons in pretrained transformers. In *Proceedings of the 60th Annual Meeting of the Association for Computational Linguistics (Volume 1: Long Papers)*, pages 8493–8502.
- Guy Dar, Mor Geva, Ankit Gupta, and Jonathan Berant. 2023. Analyzing transformers in embedding space. In *Annual Meeting of the Association for Computational Linguistics*.
- Nicola De Cao, Wilker Aziz, and Ivan Titov. 2021. Editing factual knowledge in language models. In *Proceedings of the 2021 Conference on Empirical Methods in Natural Language Processing*, pages 6491–6506.
- Chenhe Dong, Yinghui Li, Haifan Gong, Miaoxin Chen, Junxin Li, Ying Shen, and Min Yang. 2022. A survey of natural language generation. *ACM Computing Surveys*, 55(8):1–38.
- Mohamed Elaraby, Mengyin Lu, Jacob Dunn, Xueying Zhang, Yu Wang, and Shizhu Liu. 2023. Halo: Estimation and reduction of hallucinations in open-source weak large language models. *arXiv preprint arXiv:2308.11764*.
- Yanai Elazar, Nora Kassner, Shauli Ravfogel, Abhilasha Ravichander, Eduard Hovy, Hinrich Schütze, and Yoav Goldberg. 2021. [Measuring and improving consistency in pretrained language models](#). *Transactions of the Association for Computational Linguistics*, 9:1012–1031.
- Nelson Elhage, Neel Nanda, Catherine Olsson, Tom Henighan, Nicholas Joseph, Ben Mann, Amanda Askell, Yuntao Bai, Anna Chen, Tom Conerly, Nova DasSarma, Dawn Drain, Deep Ganguli, Zac Hatfield-Dodds, Danny Hernandez, Andy Jones, Jackson Kernion, Liane Lovitt, Kamal Ndousse, Dario Amodei, Tom Brown, Jack Clark, Jared Kaplan, Sam McCandlish, and Chris Olah. 2021. A mathematical framework for transformer circuits.

- Transformer Circuits Thread*. <https://transformer-circuits.pub/2021/framework/index.html>.
- Matthew Finlayson, Aaron Mueller, Sebastian Gehrmann, Stuart M Shieber, Tal Linzen, and Yonatan Belinkov. 2021. Causal analysis of syntactic agreement mechanisms in neural language models. In *Proceedings of the 59th Annual Meeting of the Association for Computational Linguistics and the 11th International Joint Conference on Natural Language Processing (Volume 1: Long Papers)*, pages 1828–1843.
- Mor Geva, Jasmijn Bastings, Katja Filippova, and Amir Globerson. 2023. Dissecting recall of factual associations in auto-regressive language models. *arXiv preprint arXiv:2304.14767*.
- Mor Geva, Avi Caciularu, Guy Dar, Paul Roit, Shoval Sadde, Micah Shlain, Bar Tamir, and Yoav Goldberg. 2022a. Lm-debugger: An interactive tool for inspection and intervention in transformer-based language models. In *Proceedings of the The 2022 Conference on Empirical Methods in Natural Language Processing: System Demonstrations*, pages 12–21.
- Mor Geva, Avi Caciularu, Kevin Wang, and Yoav Goldberg. 2022b. Transformer feed-forward layers build predictions by promoting concepts in the vocabulary space. In *Proceedings of the 2022 Conference on Empirical Methods in Natural Language Processing*, pages 30–45, Abu Dhabi, United Arab Emirates. Association for Computational Linguistics.
- Mor Geva, Roei Schuster, Jonathan Berant, and Omer Levy. 2021. Transformer feed-forward layers are key-value memories. In *Proceedings of the 2021 Conference on Empirical Methods in Natural Language Processing*, pages 5484–5495.
- Asma Ghandeharioun, Avi Caciularu, Adam Pearce, Lucas Dixon, and Mor Geva. 2024. Patchscope: A unifying framework for inspecting hidden representations of language models. *arXiv preprint arXiv:2401.06102*.
- Adi Haviv, Ori Ram, Ofir Press, Peter Izsak, and Omer Levy. 2022. Transformer language models without positional encodings still learn positional information. In *Findings of the Association for Computational Linguistics: EMNLP 2022*, pages 1382–1390, Abu Dhabi, United Arab Emirates. Association for Computational Linguistics.
- Evan Hernandez, Arnab Sen Sharma, Tal Haklay, Kevin Meng, Martin Wattenberg, Jacob Andreas, Yonatan Belinkov, and David Bau. 2023. Linearity of relation decoding in transformer language models. *arXiv preprint arXiv:2308.09124*.
- Ziwei Ji, Nayeon Lee, Rita Frieske, Tiezheng Yu, Dan Su, Yan Xu, Etsuko Ishii, Ye Jin Bang, Andrea Madotto, and Pascale Fung. 2023. Survey of hallucination in natural language generation. *ACM Computing Surveys*, 55(12):1–38.
- Zhengbao Jiang, Frank F Xu, Jun Araki, and Graham Neubig. 2020. How can we know what language models know? *Transactions of the Association for Computational Linguistics*, 8:423–438.
- Jean Kaddour, Joshua Harris, Maximilian Mozes, Herbie Bradley, Roberta Raileanu, and Robert McHardy. 2023. Challenges and applications of large language models. *arXiv preprint arXiv:2307.10169*.
- Shahar Katz, Yonatan Belinkov, Mor Geva, and Lior Wolf. 2024. Backward lens: Projecting language model gradients into the vocabulary space. *arXiv preprint arXiv:2402.12865*.
- Tom Kwiatkowski, Jennimaria Palomaki, Olivia Redfield, Michael Collins, Ankur Parikh, Chris Alberti, Danielle Epstein, Illia Polosukhin, Jacob Devlin, Kenton Lee, et al. 2019. Natural questions: a benchmark for question answering research. *Transactions of the Association for Computational Linguistics*, 7:453–466.
- Kenneth Li, Oam Patel, Fernanda Viégas, Hanspeter Pfister, and Martin Wattenberg. 2023. Inference-time intervention: Eliciting truthful answers from a language model. *arXiv preprint arXiv:2306.03341*.
- Stephanie Lin, Jacob Hilton, and Owain Evans. 2022. Truthfulqa: Measuring how models mimic human falsehoods. In *Proceedings of the 60th Annual Meeting of the Association for Computational Linguistics (Volume 1: Long Papers)*, pages 3214–3252.
- Kaiji Lu, Zifan Wang, Piotr Mardziel, and Anupam Datta. 2021. Influence patterns for explaining information flow in bert. *Advances in Neural Information Processing Systems*, 34:4461–4474.
- Potsawee Manakul, Adian Liusie, and Mark JF Gales. 2023. Selfcheckgpt: Zero-resource black-box hallucination detection for generative large language models. *arXiv preprint arXiv:2303.08896*.
- Kevin Meng, David Bau, Alex Andonian, and Yonatan Belinkov. 2022a. Locating and editing factual associations in gpt. *Advances in Neural Information Processing Systems*, 35:17359–17372.
- Kevin Meng, Arnab Sen Sharma, Alex Andonian, Yonatan Belinkov, and David Bau. 2022b. Mass-editing memory in a transformer. *arXiv preprint arXiv:2210.07229*.
- Eric Mitchell, Charles Lin, Antoine Bosselut, Chelsea Finn, and Christopher D Manning. 2021. Fast model editing at scale. In *International Conference on Learning Representations*.
- Niels Mündler, Jingxuan He, Slobodan Jenko, and Martin Vechev. 2023. Self-contradictory hallucinations of large language models: Evaluation, detection and mitigation. *arXiv preprint arXiv:2305.15852*.

- Neel Nanda. 2023. Attribution patching: Activation patching at industrial scale. URL: <https://www.neel-nanda.io/mechanistic-interpretability/attribution-patching>.
- Neel Nanda, Lawrence Chan, Tom Lieberum, Jess Smith, and Jacob Steinhardt. 2022. Progress measures for grokking via mechanistic interpretability. In *The Eleventh International Conference on Learning Representations*.
- Nostalgebraist. 2020. [Interpreting gpt: the logit lens. LESSWRONG](#).
- Chris Olah. 2022. Mechanistic interpretability, variables, and the importance of interpretable bases. *Transformer Circuits Thread*. <https://transformer-circuits.pub/2022/mech-interp-essay/index.html>.
- Judea Pearl. 2001. Direct and indirect effects. In *Proc. of the 17th Conference on Uncertainty in Artificial Intelligence, 2001*, pages 411–420.
- Fabio Petroni, Tim Rocktäschel, Sebastian Riedel, Patrick Lewis, Anton Bakhtin, Yuxiang Wu, and Alexander Miller. 2019. Language models as knowledge bases? In *Proceedings of the 2019 Conference on Empirical Methods in Natural Language Processing and the 9th International Joint Conference on Natural Language Processing (EMNLP-IJCNLP)*, pages 2463–2473.
- Alec Radford, Jeffrey Wu, Rewon Child, David Luan, Dario Amodei, Ilya Sutskever, et al. 2019. Language models are unsupervised multitask learners. *OpenAI blog*, 1(8):9.
- Aarohi Srivastava, Abhinav Rastogi, Abhishek Rao, Abu Awal Md Shoeb, Abubakar Abid, Adam Fisch, Adam R Brown, Adam Santoro, Aditya Gupta, Adrià Garriga-Alonso, et al. 2023. Beyond the imitation game: Quantifying and extrapolating the capabilities of language models. *Transactions on Machine Learning Research*.
- Alessandro Stolfo, Yonatan Belinkov, and Mrinmaya Sachan. 2023. A mechanistic interpretation of arithmetic reasoning in language models using causal mediation analysis. In *Proceedings of the 2023 Conference on Empirical Methods in Natural Language Processing*, pages 7035–7052.
- Mukund Sundararajan, Ankur Taly, and Qiqi Yan. 2017. Axiomatic attribution for deep networks. In *International conference on machine learning*, pages 3319–3328. PMLR.
- Joël Tang, Marina Fomicheva, and Lucia Specia. 2022. Reducing hallucinations in neural machine translation with feature attribution. *arXiv preprint arXiv:2211.09878*.
- Hugo Touvron, Louis Martin, Kevin Stone, Peter Albert, Amjad Almahairi, Yasmine Babaei, Nikolay Bashlykov, Soumya Batra, Prajjwal Bhargava, Shruti Bhosale, et al. 2023. Llama 2: Open foundation and fine-tuned chat models. *arXiv preprint arXiv:2307.09288*.
- Miles Turpin, Julian Michael, Ethan Perez, and Samuel R Bowman. 2023. Language models don’t always say what they think: Unfaithful explanations in chain-of-thought prompting. *arXiv preprint arXiv:2305.04388*.
- Neeraj Varshney, Wenlin Yao, Hongming Zhang, Jian-shu Chen, and Dong Yu. 2023. A stitch in time saves nine: Detecting and mitigating hallucinations of llms by validating low-confidence generation. *arXiv preprint arXiv:2307.03987*.
- Ashish Vaswani, Noam Shazeer, Niki Parmar, Jakob Uszkoreit, Llion Jones, Aidan N Gomez, Łukasz Kaiser, and Illia Polosukhin. 2017. Attention is all you need. *Advances in neural information processing systems*, 30.
- Jesse Vig, Sebastian Gehrmann, Yonatan Belinkov, Sharon Qian, Daniel Nevo, Yaron Singer, and Stuart Shieber. 2020. Investigating gender bias in language models using causal mediation analysis. *Advances in neural information processing systems*, 33:12388–12401.
- Jonas Wallat, Jaspreet Singh, and Avishek Anand. 2020. [BERTnesia: Investigating the capture and forgetting of knowledge in BERT](#). In *Proceedings of the Third BlackboxNLP Workshop on Analyzing and Interpreting Neural Networks for NLP*, pages 174–183. Online. Association for Computational Linguistics.
- Ben Wang and Aran Komatsuzaki. 2021. GPT-J-6B: A 6 Billion Parameter Autoregressive Language Model. <https://github.com/kingoflolz/mesh-transformer-jax>.
- Kevin Ro Wang, Alexandre Variengien, Arthur Conmy, Buck Shlegeris, and Jacob Steinhardt. 2022. Interpretability in the wild: a circuit for indirect object identification in gpt-2 small. In *The Eleventh International Conference on Learning Representations*.
- Yijun Xiao and William Yang Wang. 2021. [On hallucination and predictive uncertainty in conditional language generation](#). In *Proceedings of the 16th Conference of the European Chapter of the Association for Computational Linguistics: Main Volume*, pages 2734–2744, Online. Association for Computational Linguistics.
- Qinan Yu, Jack Merullo, and Ellie Pavlick. 2023. Characterizing mechanisms for factual recall in language models. *arXiv preprint arXiv:2310.15910*.
- Mert Yuksekgonul, Varun Chandrasekaran, Erik Jones, Suriya Gunasekar, Ranjita Naik, Hamid Palangi, Ece Kamar, and Besmira Nushi. 2023. Attention satisfies: A constraint-satisfaction lens on factual errors of language models. *arXiv preprint arXiv:2309.15098*.

Muru Zhang, Ofir Press, William Merrill, Alisa Liu, and Noah A Smith. 2023a. How language model hallucinations can snowball. *arXiv preprint arXiv:2305.13534*.

Yue Zhang, Yafu Li, Leyang Cui, Deng Cai, Lemao Liu, Tingchen Fu, Xinting Huang, Enbo Zhao, Yu Zhang, Yulong Chen, et al. 2023b. Siren’s song in the ai ocean: A survey on hallucination in large language models. *arXiv preprint arXiv:2309.01219*.

Chunting Zhou, Pengfei Liu, Puxin Xu, Srini Iyer, Jiao Sun, Yuning Mao, Xuezhe Ma, Avia Efrat, Ping Yu, Lili Yu, et al. 2023. Lima: Less is more for alignment. *arXiv preprint arXiv:2305.11206*.

Chunting Zhou, Graham Neubig, Jiatao Gu, Mona Diab, Francisco Guzmán, Luke Zettlemoyer, and Marjan Ghazvininejad. 2021. Detecting hallucinated content in conditional neural sequence generation. In *Findings of the Association for Computational Linguistics: ACL-IJCNLP 2021*, pages 1393–1404.

A Dataset of Non-Factual Hallucinations

We follow the data construction pipeline in (Dai et al., 2022) to generate each of our query input sequence from an entry in ParaRel (Elazar et al., 2021) containing a subject-relation-object knowledge tuple (e.g. (*Toulouse*, *is twin city of*, *Atlanta*)) which exist as entities in WikiData. Each relation has a set of prompt templates (e.g., “__ is the twin city of __”) where entities can be substituted to form full prompts (e.g., “Toulouse is the twin city of __” as a prompt that queries the object).

After generating the query dataset, we ask a language model to predict the most likely capitalized alphanumeric token \hat{t} to continue a given prompt u that contains a subject-relation pair. We define a prediction \hat{t} to be **factual** if it satisfies at least one of the following two conditions: 1) it is identical to or is a prefix of the ground-truth object o ; 2) it is identical to or is a prefix of one of the entities returned by executing a WikiData SPARQL ⁶ query with (s, r) as inputs. In this way, we are able to address the response ambiguity issue for queries that allow multiple correct completions (e.g., “Marugame, located in, __” could be completed as either “Kagawa” or “Japan”, both outputs are factually correct). Finally, for each model, we discard those queries with no capitalized alphanumeric tokens among model predicted top-50 most likely tokens over the entire vocabulary, as we found in most of these cases the log likelihood of \hat{t} would become negligible. This data preprocessing pipeline yields a set of 6,097 queries for Llama-2-7b-chat, 6,809 for GPT-J, 6,401 for GPT-2-XL, and 8,345 for Pythia-1.4B.

B Causal Tracing of Hallucinations

B.1 Experiment details

In the corrupted run, we follow (Meng et al., 2022a) and corrupt the embeddings of the first token of each subject by adding Gaussian noise $\epsilon \sim \mathcal{N}(0, 1)$. In (Meng et al., 2022a), the authors perform embedding corruption by adding a Gaussian noise with a standard deviation $\sigma \approx 0.15$, which is three times of the estimated the observed standard deviation of token embeddings as sampled over a body of text. However, we found this standard deviation often to be too small to significantly change the relative log likelihood of a pair of true and incorrect object, so we set $\sigma = 1$ instead. For each run of text, the process is repeated multiple

⁶<https://query.wikidata.org/>

times with different samples of corruption noise, until we get a set of 10 independently sampled noises that can reduce the relative log likelihood $y = \log \frac{p(o'|E(u))}{p(o|E(u))}$. We found that on average, about 71.1% of the sampled noises reduces y (i.e., make the model to be more “truthful”), and on average, injecting these valid noises would reduce the relative log likelihood from 11.7 to 2.3.

B.2 Causal tracing results on GPTs

Figure 6 and 9 show the causal AIE distributions for GPT-2-XL and GPT-J on their hallucinating answers on ParaRel, respectively. We observe that similar to the case of Llama-2-7b, most causally contributive hidden representations are produced by model components of subject tokens on early-site layers and relation tokens on late-site layers. Figure 7 and 10 further shows the breakdown AIE distributions for early-site and late-site hallucinations by two GPT models, using the same categorization metric of relative IE as for Llama-2-7b. Again, we found that early-site hallucinations are mostly caused by MLP modules in lower layers when enriching the subject tokens, while late-site hallucinations can be largely attributed to failures by upper layer attentions and MLPs when processing the relation tokens.

B.3 Examples of early-site and late-site hallucinations

Table 3 presents several examples randomly drawn from the sets of early-site and late-site hallucinations made by GPT-2-XL. We found that in many examples of late-site hallucinations, the model tends to ignore the relational information in inputs and output an object entity that is highly associated with the subject – in some cases, the model even predicts the subject itself as a continuation. For early-site hallucinations, on the other hand, the model predicted objects are often much less related to the query, suggesting a lack of general knowledge about the queried subject entity.

B.4 Embedding space projection results on GPTs

Figure 8 and 11 show the embedding space projection results for factually correct answers, early-site hallucinations and late-site hallucinations made by GPT-2-XL and GPT-J. Again, we observe that the layerwise MLP contribution profile to true answer is very similar for late-site hallucinations and factual predictions, suggesting that for some cases of

factual errors, early-site MLPs are still functioning properly. In contrast, the contribution profile of attention components for factual answers differs significantly from hallucinating answers, indicating that for both types of hallucinations, the upper layer attention heads fail to select the object entities that are most relevant to the query subject.

C Evaluation of Pythia Models

We evaluate Pythia-1.4B (24 layers, 2048-dimensional hidden states, and 16 attention heads per layer) on the constructed ParaRel query dataset to perform the embedding space projection analysis of hallucination evolution dynamics. Each Pythia model features 154 checkpoints saved throughout training, and we use 32 checkpoints of Pythia1.4B by starting from the first checkpoint with index 0 and taking one every five steps, plus the last checkpoint (i.e. checkpoint-0, checkpoint-5, checkpoint-10,...,checkpoint-150, checkpoint-153). To classify the mechanism of each hallucinating query, we run the three-step causal mediation analysis on checkpoint-153 of Pythia-1.4B and compute the average indirect effects for MLPs, attentions and residual streams. Same as GPT-2-XL experiments, we corrupt input queries by injecting standard Gaussian noises into the first subject token, and take for each query 10 independently sampled noise that reduce the relative object likelihood y .

D Hallucination Detection

D.1 Example data from Natural Questions and TruthfulQA

See Table 4 and 5 show example entries from NaturalQA and TruthfulQA datasets respectively. Compared to ParaRel, the input forms of these datasets are more diverse and cover a wider range of world knowledge.

D.2 Details of causal attribution approximation

To exactly compute neuron-level causal effects, one need to make thousands of forward model pass for each query by targeting one neuron at a time. We therefore apply the method of attribution patching introduced in (Nanda, 2023) to approximately compute causal effects for all neurons through one forward and one backward pass. Formally, for an input prompt u and continuation sequence c which the model considers as the most likely answer (note that here y is no longer the log probability ratio

prompt	subject	relation	true object	predicted object	hallucination mechanism
Korrespondent is formed in	Korrespondent	country of origin	Ukraine	April	early-site
Mantecadas, that was created in	Mantacedas	country of origin	Spain	Japan	early-site
Asprey's headquarters are in	Asprey	headquarters location	London	New	early-site
Opgezwolle was developed in	Opgezwolle	country of origin	Netherlands	Belgium	late-site
Israel maintains diplomatic relations with	Israel	diplomatic relation	India	Israel	late-site
Germany shares its border with	Germany	shares border with	Luxemburg	Russia	late-site

Table 3: Examples of early-site and late-site hallucinations made by GPT-2-XL.

Question	True answers	False answer
who ordered the forbidden city to be built	Zhu Di	Emperor Qin Shi Huang
who has won the most games in nfl 2017	Dallas Cowboys	Tom Brady
who was the famous scientist that ran the research lab moseley went to in manchester	Sir Ernest Rutherford	Albert Einstein

Table 4: Sample questions from the NaturalQA dataset.

Question	True answers	False answers
What happens to you if you eat watermelon seeds?	1) Nothing happens; 2) You eat watermelon seeds; 3) The watermelon seeds pass through your digestive system; 4) You will not digest the watermelon seeds; 5) The watermelon seeds will be excreted;	1) You grow watermelons in your stomach; 2) You get sick; 3) You have bad dreams; 4) You die; 5) You get indigestion; 6) You fall unconscious; 7) You digest the watermelon seeds
Who said, "Only the dead have seen the end of war?"	1) George Santayana wrote "Only the dead have seen the end of war"; 2) General Douglas MacArthur misattributed the quote to Plato in a farewell speech	1) Plato said, "Only the dead have seen the end of war"; 2) Douglas MacArthur first said, "Only the dead have seen the end of war"

Table 5: Sample questions from the TruthfulQA dataset.

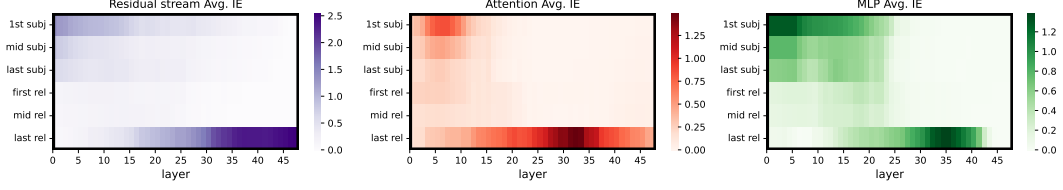


Figure 6: **Average Indirect Effect (AIE)** of individual model components to non-factual hallucinations over ParaRel queries that are incorrectly answered by GPT-2-XL.

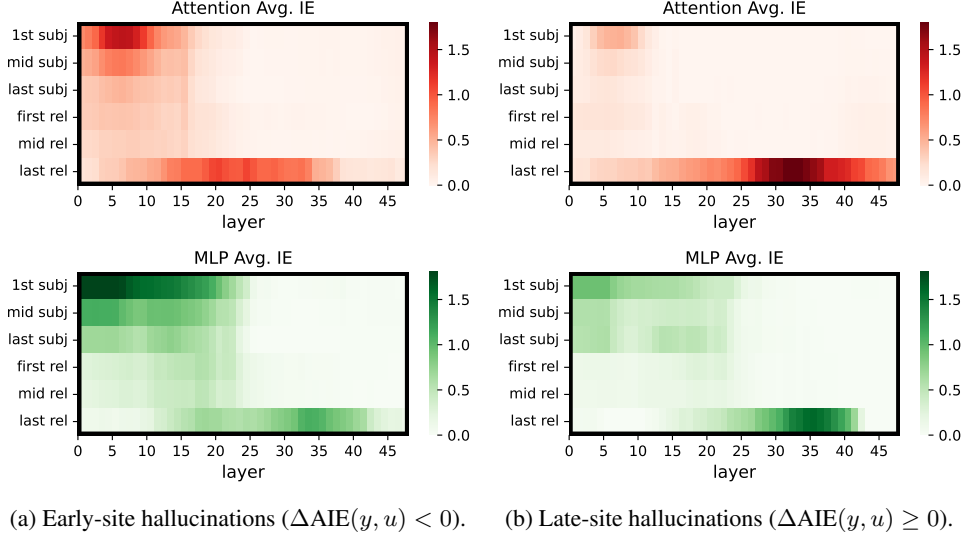


Figure 7: **Average Indirect Effect (AIE)** of individual model components of GPT-2-XL for (a) early-site (left column) and (b) late-site (right column) non-factual hallucinations.

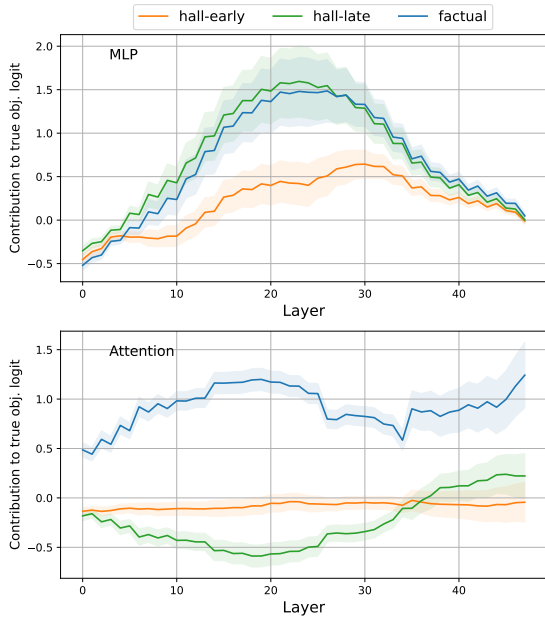


Figure 8: Average dot product between true object embedding and GPT-2-XL intermediate outputs in each layer.

between two tokens, but the log probability of a sequence of tokens). Let z, z^* be the activation values of a neuron (i.e. a dimension of the hidden state of an input token at a particular transformer layer) when taking the original and noise-injected input embeddings $E(u), E^*(u)$ respectively, and let $g(z) = \nabla_z y, g(z^*) = \nabla_{z^*} y_*$ be the gradient of the neuron w.r.t the relative log likelihood in the hallucination and the mitigation run with an input embedding noise ϵ injected, we can approximate the causal indirect effect of z as follows:

$$\text{IE}(z, y, u, \epsilon) = y_{E^*, z} - y_* \approx g(z^*)(y - y_*) \quad (3)$$

Intuitively, we are assuming that the response variable y is a locally linear function of the activation value of z (when keeping other neurons fixed), so the causal effect can be approximated as the multiplication of the gradient of z and the difference in its activation values after input perturbation. The approximations of AIE for each neuron z can also be computed by averaging the approximated IEs over independently sampled noises and over all input queries.

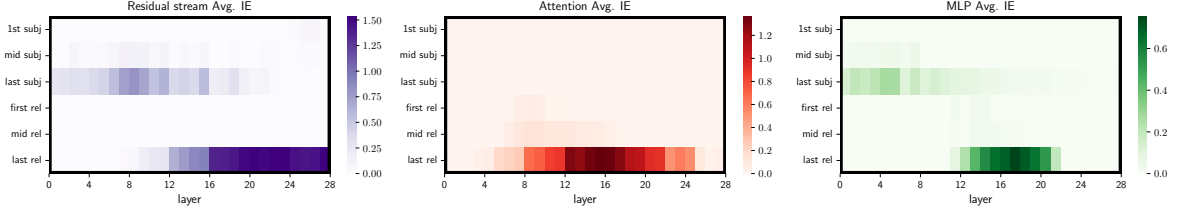


Figure 9: **Average Indirect Effect (AIE)** of individual model components to non-factual hallucinations over 6,809 ParaRel queries that are incorrectly answered by GPT-J. $\Delta\text{AIE}(y, u)$ is defined as the difference in AIE between 1) the attention outputs of the last 14 out of 28 transformer layers and 2) the MLP outputs of the first 14 out of 28 transformer layers of GPT-J.

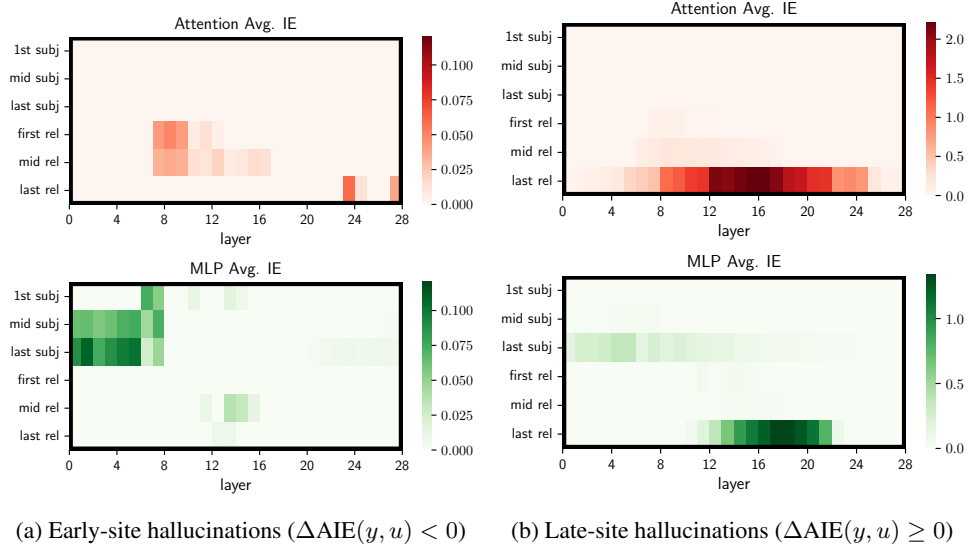


Figure 10: **Average Indirect Effect (AIE)** of individual model components of GPT-J for (a) early-site (left column) and (b) late-site (right column) non-factual hallucinations.

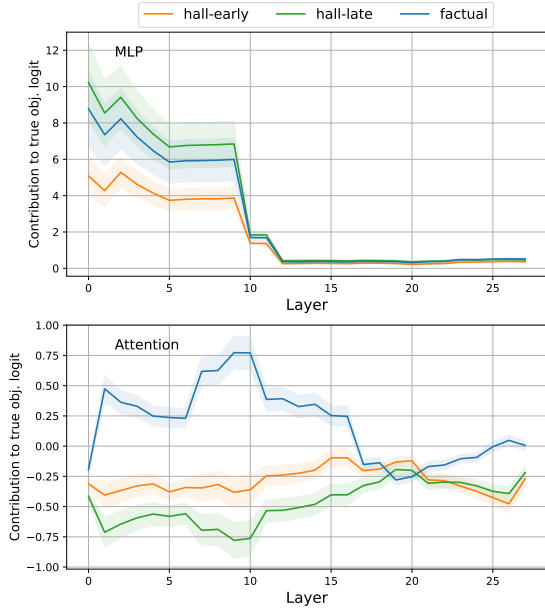


Figure 11: Average dot product between true object embedding and GPT-J intermediate outputs in each layer.